GMR
The Original

# MULTIFUNCTIONAL BIOCOMPATIBLE FABRICATION OF NOVEL STARCH/PVA/CuO ELECTROSPUN NANOSCAFFOLDS FROM *Sargassum ilicifolium* (BROWN MARINE MACROALGAE) EXTRACT: PHYSICOCHEMICAL CHARACTERIZATION AND ANTIDIABETIC ASSESSMENT

**Vanama Saketh Saran[1], Keerthana Muthukumaran[2], Ramganesh Selvarajan[3]***

[1]Saveetha Medical College & Hospital (SMCH), Saveetha Institute of Medical and Technical Sciences (SIMATS), Thandalam, Chennai, Tamil Nadu 602105, India. sakethvanama123@gmail.com
[2]Department of Dermatology, Saveetha Medical College & Hospital (SMCH), Saveetha Institute of Medical and Technical Sciences (SIMATS), Thandalam, Chennai, Tamil Nadu 602105, India. keerthi98muthukumaran@gmail.com
[3]Centre for Microbial Ecology and Translational Research, Department of Microbiology, Saveetha Medical College and Hospital, Saveetha Institute of Medical And Technical Sciences (SIMATS), Thandalam, Chennai-602105, Tamil Nadu, India. Email: ramganesh.presidency@gmail.com
***Correspondence Author:** Ramganesh Selvarajan, ramganesh.presidency@gmail.com (R.S.)

**ABSTRACT**
The present study reports the eco-friendly synthesis of copper oxide (CuO) nanoparticles using *Sargassum ilicifolium* extract and their integration into starch/polyvinyl alcohol (PVA)-based electrospun nanoscaffolds for potential antidiabetic applications. The biosynthesized CuO nanoparticles were thoroughly characterized using UV–Vis spectroscopy, Fourier Transform Infrared Spectroscopy (FTIR), X-Ray Diffraction (XRD), Scanning Electron Microscopy (SEM), Thermogravimetric Analysis (TGA), and DLS analyses, confirming their nanoscale size, crystalline nature, thermal stability, and functional group interactions. The fabricated nanoscaffolds exhibited a smooth, uniform fibrous architecture with enhanced stability and dispersion of CuO nanoparticles. *In vitro* biological assays demonstrated significant inhibitory activity of the starch/PVA/CuO-NPs nanoscaffolds against α-amylase and α-glucosidase enzymes, indicating strong antidiabetic potential. Compared to individual components, the composite scaffold showed superior bioactivity, likely due to the synergistic effect of the biopolymer matrix and embedded nanoparticles. This green nanotechnological approach provides a promising route for the development of sustainable, biocompatible therapeutic scaffolds. Overall, the study highlights the potential of marine algae-mediated nanoparticle synthesis and biopolymer-based scaffolding for use in diabetes management and other biomedical applications. Further studies, including *in vivo* evaluations, are essential to validate these findings and explore the clinical applicability of the developed nanomaterials.

**KEYWORDS:** *Sargassum ilicifolium*, Green synthesis, CuO NPs, Starch/PVA/CuO-NPs nanoscaffolds, Antidiabetic activity.

## 1. INTRODUCTION

Diabetes mellitus, a complex metabolic disorder characterized by chronic hyperglycemia, continues to pose a global health challenge [1]. It results primarily from impaired insulin secretion, action, or both, leading to systemic complications such as neuropathy, retinopathy, nephropathy, and cardiovascular diseases [2]. According to the International Diabetes Federation (IDF), over 537 million adults were estimated to live with diabetes in 2021, with projections reaching 783 million by 2045 [3]. Despite the availability of synthetic antidiabetic drugs, their long-term use is often associated with undesirable side effects, limited efficacy, and high costs, especially in low-resource settings [4]. These limitations have accelerated the global pursuit of natural and biocompatible alternatives, particularly from marine sources, for safer and more effective diabetes management [5].

Marine algae, especially brown macroalgae such as *Sargassum ilicifolium*, have gained considerable attention in recent years for their rich reservoir of bioactive compounds, including phlorotannins, polysaccharides, fucoidans, and polyphenols [6]. These compounds exhibit diverse therapeutic properties such as antioxidant, antimicrobial, antitumor, and notably, antidiabetic activities [7]. *S. ilicifolium*, commonly found along the Indian coastline, is a prominent species known for its traditional medicinal usage and its role in folk remedies [8]. With advancements in extraction technologies, particularly ultrasonic-assisted extraction (UAE), the recovery of thermolabile and structurally complex phytochemicals from macroalgae has become significantly more efficient [9]. UAE enhances cellular disruption through cavitation, thereby improving the bioactive yield without requiring elevated temperatures that might degrade sensitive compounds [10].

Concurrently, green nanotechnology has emerged as a transformative approach to synthesize nanoparticles using biological systems [11]. The eco-friendly synthesis of metal and metal oxide nanoparticles through algal extracts

represents a sustainable alternative to conventional chemical routes, which often involve toxic solvents and high energy inputs [12]. Among various metal oxides, copper oxide nanoparticles (CuO NPs) have demonstrated compelling therapeutic potential due to their antioxidant, antimicrobial, anticancer, and antidiabetic properties [13]. The use of marine algae as a reducing and stabilizing agent in nanoparticle synthesis not only ensures biocompatibility but also incorporates the synergistic benefits of marine-derived phytoconstituents [14].

In recent biomedical research, biopolymeric scaffolds embedded with bioactive nanoparticles have gained prominence for targeted drug delivery, tissue engineering, and chronic disease management [15]. Electrospinning, a versatile technique for producing nanofibrous scaffolds, allows the fabrication of ultrafine fibers with high surface-area-to-volume ratios, tunable porosity, and morphological similarity to the natural extracellular matrix (ECM) [16]. Such properties are essential for enhancing cell adhesion, proliferation, and sustained release of incorporated therapeutic agents [16]. Starch and polyvinyl alcohol (PVA) are two biocompatible polymers frequently utilized in scaffold design [17]. Starch, a natural polysaccharide, offers advantages such as biodegradability and non-toxicity, while PVA contributes mechanical stability, flexibility, and hydrophilicity to the composite scaffold [18].

The integration of CuO NPs into a starch/PVA nanofiber matrix using electrospinning can potentially create a multifunctional scaffold that exhibits structural integrity, biocompatibility, and therapeutic efficacy [19]. However, the novelty of the present work lies not only in the fabrication of such a composite but also in the green synthesis route employed [20]. Herein, CuO NPs are biosynthesized using *S. ilicifolium* extract through a rapid and scalable ultrasonic-assisted approach, which minimizes environmental impact and preserves the therapeutic essence of the biological material [21]. Embedding these algal-mediated CuO NPs within a starch/PVA nanoscaffold allows for the controlled and sustained release of bioactive molecules, which is particularly advantageous for diabetic wound care and systemic glucose regulation [19].

Moreover, the functional characterization of nanoparticles and nanofibrous mats is pivotal for validating their suitability for biomedical applications [22]. Techniques such as UV–Vis spectroscopy, Fourier Transform Infrared Spectroscopy (FTIR), X-Ray Diffraction (XRD), Scanning Electron Microscopy (SEM), Thermogravimetric Analysis (TGA), and zeta potential analysis offer insights into the physicochemical, thermal, and morphological features of the synthesized materials [23]. These characterizations ensure the structural integrity, thermal stability, and uniform dispersion of nanoparticles within the polymeric matrix, all of which influence the scaffold's performance in biological environments [24].

An equally significant aspect of this study is the biological assessment of antidiabetic activity via *in vitro* enzymatic inhibition assays [25]. Enzymes like α-amylase and α-glucosidase play a critical role in the hydrolysis of carbohydrates into glucose [26]. Inhibiting these enzymes helps regulate postprandial blood glucose levels, a key strategy in managing type 2 diabetes [27]. Natural α-amylase and α-glucosidase inhibitors derived from marine macroalgae have shown promise as effective alternatives to synthetic drugs like acarbose [28]. In this study, the antidiabetic efficacy of *S. ilicifolium* extract, biosynthesized CuO NPs, and the electrospun starch/PVA/CuO nanoscaffold is systematically evaluated using these enzymatic inhibition assays.

The novelty and scientific contribution of this work are multifaceted. First, it employs *S. ilicifolium*, an underutilized yet bioresource-rich brown alga, for the biogenic synthesis of CuO NPs using an ultrasonic-assisted method, which enhances extraction efficiency while maintaining ecological sustainability. Second, the synthesized nanoparticles are embedded within a dual-polymer (starch/PVA) electrospun nanoscaffold to produce a multifunctional biomaterial with potential applications in diabetes management and diabetic wound healing. Third, the nanocomposite scaffold is characterized comprehensively for its physicochemical and morphological features to ensure biomedical compatibility. Finally, the antidiabetic activity of all components is thoroughly validated through standard *in vitro* assays targeting key digestive enzymes implicated in hyperglycemia.

## 2. MATERIALS AND METHODS

### 2.1. Collection and processing of marine macroalgae

Fresh samples of the brown marine macroalga *S. ilicifolium* were carefully harvested by hand from the intertidal zones along the coastal area of Rameswaram, India. To maintain the bioactive integrity of the algae, the collected material was immediately placed in ice-cooled containers for transport to the laboratory. Upon arrival, the biomass was rinsed thoroughly with tap water to remove adhering sand, debris, and epiphytes, followed by several washes with distilled water to ensure complete purification from extraneous substances. The clean algal material was then cut into small pieces and dried under shade with good air circulation at ambient room temperature for about 14 days. Once completely desiccated, the dried seaweed was ground using a mechanical grinder to produce a fine powder, which was stored in airtight containers at room temperature for subsequent extraction procedures.

### 2.2. UAE of bioactive molecules

Bioactive compounds were extracted from *S. ilicifolium* powder via UAE to enhance yield. Exactly 2 grams of the powdered algae was mixed with 50 mL of Milli-Q water. The mixture was subjected to sonication in a LABQUEST ultrasonic cleaner (Borosil; Serial No. 941032329018) maintained at 60°C for 45 minutes. This ultrasonic treatment utilized cavitation effects to disrupt algal cell walls and facilitate the release of intracellular substances. After sonication, the extract was filtered through sterile Whatman No. 1 filter paper to remove particulate matter, resulting in a clear solution. The filtrate was kept at 10°C for immediate use and was

subsequently freeze-dried to obtain a dry extract powder suitable for storage and use in nanoparticle fabrication [29].

**2.3. Biosynthesis of CuO NPs**

CuO NPs were prepared by a green synthesis approach using the reducing agents present in the *S. ilicifolium* extract. A solution of 50 mL of 0.1 M copper sulfate pentahydrate ($CuSO4 \cdot 5H2O$) was combined with 10 mL of the algal extract (prepared by dissolving 10 mg of lyophilized powder in Milli-Q water). The mixture, maintaining a 5:1 volume ratio, was stirred continuously at 650 rpm and kept at 60°C for 2 hours. A visible color transition from blue to bluish-green confirmed the reduction of copper ions and formation of CuO NPs. The resulting suspension was centrifuged and washed thrice with double-distilled water to eliminate residual biomolecules and unreacted salts. The purified nanoparticles were freeze-dried for 48 hours and stored in a desiccator for further use in scaffold fabrication [30].

**2.4. Electrospinning of CuO-Embedded starch/PVA nanofibrous mats**

To fabricate composite nanofibrous scaffolds, a 15% (w/w) aqueous solution of PVA was prepared by dissolving PVA in Milli-Q water under constant stirring until complete dissolution was achieved. Subsequently, 100 mg each of starch and the biosynthesized CuO NPs were dispersed into this PVA solution. The mixture was stirred rigorously at 50°C for 2.5 hours to achieve homogeneous distribution and ensure proper integration of nanoparticles with the polymer matrix. The final uniform solution was loaded into a syringe fitted with a stainless-steel needle (0.84 mm internal diameter) and mounted on a HOLMARC HO-NFES-040 electrospinning machine. Electrospinning parameters were optimized as follows: voltage of 11.5 kV, a needle-to-collector distance of 12.3 cm, and a flow rate of 0.4 mL/h. The process was carried out at room temperature for 6–8 hours to produce nanofibrous mats, which were then peeled from the collector and stored under desiccated conditions for further analysis [18, 31, 32].

**2.5. Physicochemical characterization of nanoparticles and nanofibrous scaffolds**

**2.5.1. UV-Visible spectroscopy**

Optical properties and surface plasmon resonance (SPR) of the CuO NPs and *S. ilicifolium* extract were evaluated using a VIS SPEC V-730 UV-Visible spectrophotometer. Spectra were recorded between 200 and 800 nm using deionized water as the blank. Absorption peaks characteristic of nanoparticle formation were analyzed [33].

**2.5.2. FTIR spectroscopy analysis**

Functional group identification was conducted using FTIR spectroscopy in Attenuated Total Reflectance (ATR) mode with a PerkinElmer Spectrum Two instrument. Spectra for CuO NPs and the composite scaffolds were recorded over 4000–400 $cm^{-1}$ at a resolution of 4 $cm^{-1}$, averaging 64 scans per sample. The data provided insights into the interaction of functional groups such as phenolics, hydroxyls, carbonyls, and metal-oxygen bond [34].

**2.5.3. XRD analysis**

Crystallographic structure and phase purity of CuO NPs and scaffold composites were determined using a Bruker D8 Advance XRD system with CuKα radiation ($\lambda = 1.5406$ Å), operating at 40 kV and 40 mA. Diffraction patterns were recorded over 2θ angles from 5° to 90° with a step size of 0.029649°. Phase analysis was performed by comparing peaks with standard JCPDS reference files [35].

**2.5.4. SEM analysis**

Morphological characterization of nanoparticles and nanofibrous scaffolds was performed using a JEOL JSM-IT800 NANO scanning electron microscope. Prior to imaging, samples were coated with a thin gold layer via sputtering to improve conductivity. SEM images were analyzed for fiber morphology, nanoparticle distribution, and surface topology [36].

**2.5.5. TGA**

Thermal stability and decomposition profiles of the scaffolds were assessed using a PerkinElmer TGA 8000 instrument. Approximately 5 mg of sample was heated from ambient temperature to 550°C at a ramp rate of 15°C/min under nitrogen flow. Thermograms provided information on moisture loss, polymer degradation, and residual inorganic content [37].

**2.5.6. Zeta potential and particle size**

The colloidal stability and size distribution of CuO NPs were measured using a Malvern Zetasizer Ultra. Zeta potential values indicated electrostatic repulsion and nanoparticle stability in suspension, where higher absolute values corresponded to better dispersion [38].

All raw data and characterization results are accessible via the Mendeley Data repository at DOI: 10.17632/4kdtskdtmc.3.

**2.7. Assessment of antidiabetic activity**

**2.7.1. α-Amylase inhibition assay**

The inhibitory effect on α-amylase enzyme by the test samples—comprising the algal extract, CuO NPs, and starch/PVA/CuO-NPs nanoscaffolds—was determined using a modified dinitrosalicylic acid (DNSA) protocol [44]. Briefly, 200 µL of α-amylase solution (1 U/mL) was combined with 200 µL of each test formulation at different concentrations (25, 50, 75, and 100 µg/mL). This mixture was pre-incubated at 37°C for 10 minutes to facilitate interaction between enzyme and inhibitor. Following this, 200 µL of a 1% starch solution in 0.02 M sodium phosphate buffer (pH 6.9) was added, and incubation continued at 37°C for 30 minutes to allow enzymatic starch hydrolysis. The reaction was halted by adding 400 µL of DNSA reagent, and samples were heated in a water bath for 5 minutes to develop the characteristic reddish-brown color indicative of reducing sugars. After

cooling to room temperature, absorbance was measured at 540 nm with a UV–Vis spectrophotometer. Acarbose was employed as a standard inhibitor, and the half-maximal inhibitory concentration ($IC_{50}$) was calculated by plotting percentage inhibition against concentration using non-linear regression analysis [39].

**2.7.2. α-Glucosidase inhibition assay**

The α-glucosidase inhibitory capacity was evaluated through a colorimetric assay using p-nitrophenyl-α-D-glucopyranoside (pNPG) as the substrate [46]. In the assay, 50 µL of α-glucosidase enzyme solution (1 U/mL) was mixed with 50 µL of test samples at varying concentrations (25, 50, 75, and 100 µg/mL), including the algal extract, CuO NPs, and starch/PVA/CuO-NPs composite. The mixture was incubated at 37°C for 15 minutes to allow enzyme interaction. Subsequently, 50 µL of 5 mM pNPG in phosphate buffer (pH 6.8) was added, followed by further incubation at 37°C for 30 minutes to enable substrate hydrolysis. The reaction was terminated by adding 100 µL of 0.1 M sodium carbonate ($Na_2CO_3$), which facilitated the formation of a yellow chromophore due to released p-nitrophenol. Absorbance was recorded at 405 nm using a microplate reader. Acarbose served as a positive control, and $IC_{50}$ values were determined via non-linear regression to assess inhibitory strength of each test material [40, 41].

**2.8. Statistical analysis**

Data obtained from experiments were statistically analyzed using SPSS version 25.0 and GraphPad Prism 9.0 software. Results from triplicate experiments were expressed as means ± standard deviation. Differences between groups were assessed using one-way analysis of variance (ANOVA), followed by post hoc comparisons using Tukey's or Dunnett's tests as applicable. Statistical significance was set at $p < 0.05$. Relationships between variables were evaluated by Pearson's correlation coefficient, and data normality was assessed via the Shapiro-Wilk test. Non-normally distributed datasets were log-transformed where necessary. All interpretations were made within a 95% confidence interval to maintain analytical rigor [42].

## 3. RESULTS

### 3.1. UV–Visible spectroscopy

UV–Visible spectral analysis (Fig. 1) of *S. ilicifolium* extract and biosynthesized CuO NPs was conducted using a JASCO V-730 spectrophotometer over a wavelength range of 200–800 nm with 1 nm increments. The *S. ilicifolium* extract showed distinct absorption peaks at certain wavelengths, reflecting its characteristic phytochemical profile. For the CuO NPs, SPR bands were evident, confirming the formation of metal oxide nanoparticles. The spectrometer operated in continuous scan mode, with a bandwidth set at 1.0 nm and baseline corrections applied to enhance accuracy. Both samples were tested under identical parameters using deionized water as a blank. The data affirm successful CuO NPs synthesis, evident from their unique optical absorption, alongside typical spectral features of the *S. ilicifolium* extract [43].

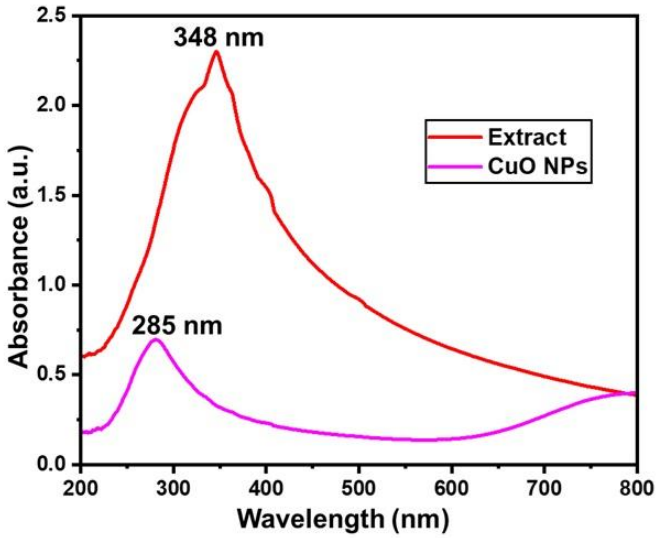


**Fig. 1. UV–Visible spectral profiles of algal extract and CuO NPs.**

### 3.2. FTIR spectroscopy analysis

FTIR spectra (Fig. 2) of CuO NPs and starch/PVA electrospun nanoscaffolds were recorded via a PerkinElmer Spectrum IR instrument employing Attenuated Total Reflectance (ATR) mode. CuO NPs exhibited key absorption peaks at 2001.38, 1651.25, 1205.19, 866.65, 599.74, and 3128.62 $cm^{-1}$, corresponding to Cu-O bond vibrations and associated surface functional groups. The starch/PVA nanoscaffolds revealed characteristic bands at 3297.43 $cm^{-1}$ (O-H stretching), 1710.65 $cm^{-1}$ (carbonyl C=O stretch), 919.77 $cm^{-1}$ (C-O-C polysaccharide stretch), and 842.91 $cm^{-1}$ (C-H bending), confirming polymeric and carbohydrate components. Spectra were acquired from 4000 to 400 $cm^{-1}$ with 4 $cm^{-1}$ resolution over 64 scans to ensure precision. Observed peak shifts and broadening suggest interactions among phenolic, hydroxyl, and carbonyl groups and successful incorporation of CuO NPs into the scaffold matrix [44-47].

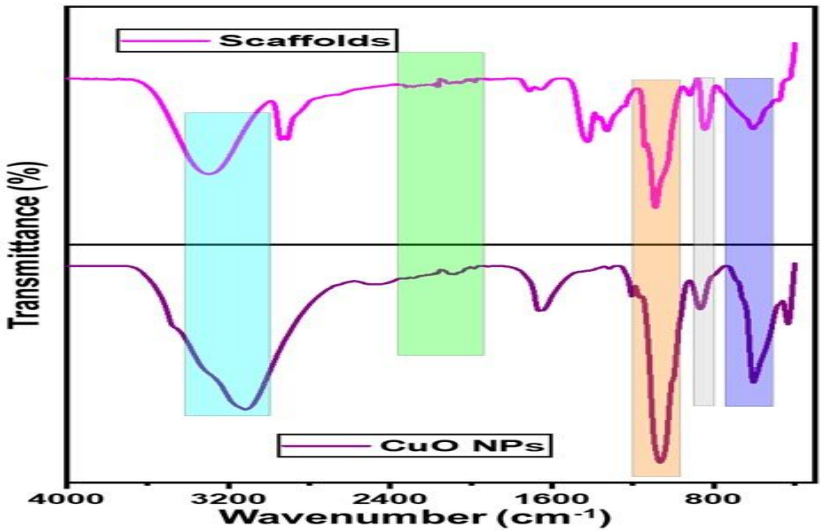


**Fig. 2. FTIR spectra of CuO NPs and their incorporation into nanoscaffolds.**

### 3.3. XRD analysis

XRD patterns (Fig. 3) of CuO NPs and starch/PVA nanoscaffolds were obtained using a Bruker D8 Advance diffractometer with CuKα radiation (λ = 1.5406 Å) at 40 kV and 40 mA. The CuO NPs showed distinct diffraction peaks at 2θ values of 16.258°, 22.278°, 26.286°, 28.070°, 29.112°, 32.792°, 37.236°, 44.982°, 48.168°, 51.879°, and 53.557°, matching the monoclinic CuO phase (JCPDS 80-1917). Crystallite sizes were calculated using the Scherrer formula. The starch/PVA scaffolds displayed peaks at 21.676°, 29.202°, 30.751°, 35.842°, 39.237°, 43.073°, 47.427°, 48.386°, and 57.535°, indicating semi-crystalline structure with d-spacings between 4.09671 Å and 1.60059 Å. The sharper and narrower peaks in CuO NPs (FWHM 0.198°–0.861°) compared to broader peaks of nanoscaffolds (FWHM 0.100°–0.658°) reflect higher crystallinity of the nanoparticles. XRD confirmed phase purity and successful integration of CuO within the nanofibers across a 2θ scan range of 5°–90°, step size 0.029649° [48-51].

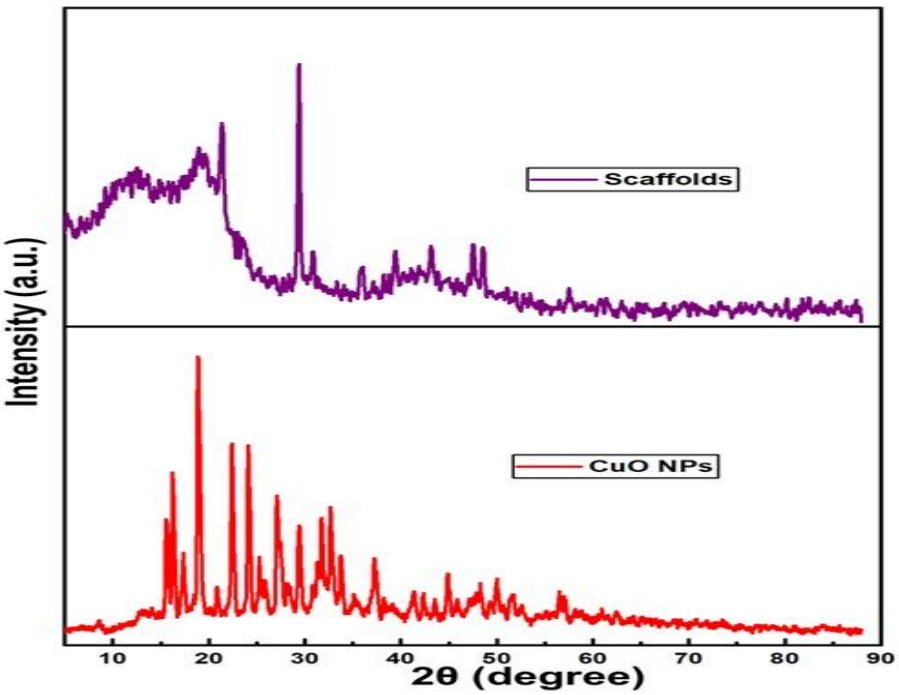


**Fig. 3. XRD patterns of synthesized CuO NPs and CuO-loaded scaffolds.**

### 3.4. SEM analysis

SEM was conducted using a JEOL JSM-IT800 NANO microscope. Samples were gold sputter-coated to enhance conductivity. SEM images (Fig. 4) of CuO NPs revealed aggregated particles varying from spherical to irregular shapes with a rough surface texture, indicating crystalline morphology. Starch/PVA electrospun nanoscaffolds exhibited an interconnected, porous fibrous network with uniform fiber diameters, confirming effective electrospinning. The fibers showed smooth surfaces with minimal bead formation, indicating homogeneous polymer blending and optimized processing parameters. These high-resolution micrographs provide essential

insight into morphology, surface characteristics, and particle distribution, supporting their suitability for biomedical and catalytic applications [52-55].

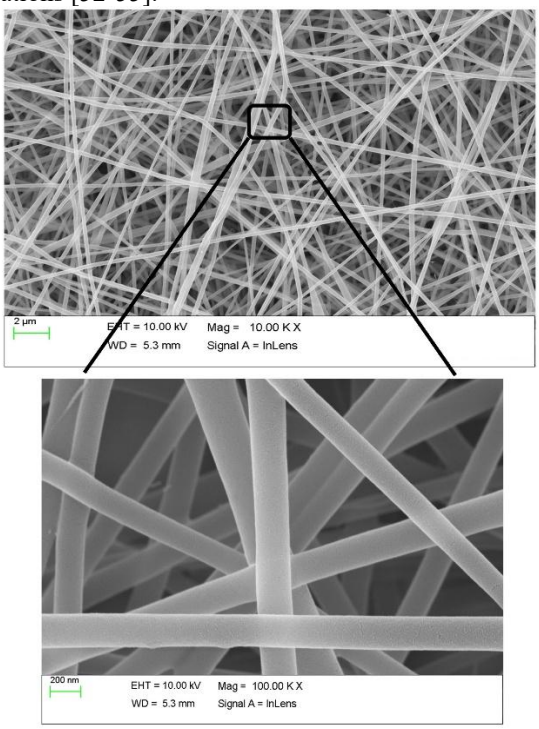


**Fig. 4. SEM analysis of synthesized CuO NPs and CuO-loaded scaffolds.**

### 3.5. TGA

TGA (Fig. 5) was performed on starch/PVA electrospun scaffolds using a PerkinElmer TGA 8000 instrument. A 3.110 mg sample was heated from 30°C to 550°C at 15°C/min. The onset of thermal degradation was observed at 232.27°C, with the maximum degradation rate at 327.56°C and completion around 374.23°C. The total weight loss recorded was 38.301%. The thermogram demonstrated an initial weight decrease due to moisture loss and polymer decomposition, followed by major degradation at elevated temperatures. These findings highlight the scaffolds' thermal stability and degradation behavior, critical for their intended functional applications [56-58].

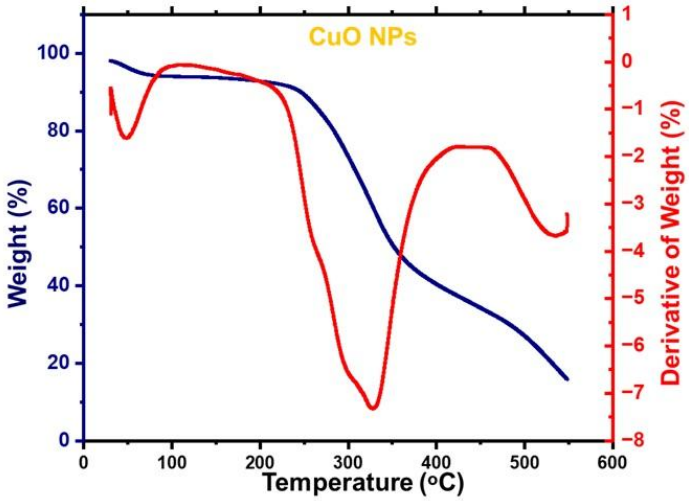


**Fig. 5. Thermal degradation behavior of CuO-incorporated nanoscaffolds.**

### 3.6. Zeta potential and particle size analysis

Dynamic Light Scattering (DLS) measurements of CuO NPs were carried out using a Malvern Zetasizer Ultra to assess particle size and colloidal stability. The average hydrodynamic diameter (Z-average) was 110 nm (Fig. 6), and the polydispersity index (PDI) was 0.7317, indicating moderate size distribution heterogeneity. Zeta potential analysis in aqueous medium at 25°C showed a mean value of −18.3 mV, with secondary peaks at −29.14 mV and −14.58 mV (Fig. 7), suggesting moderate electrostatic repulsion and dispersion stability. Suspension conductivity was measured at 0.05074 mS/cm, and the quality factor of 5.22 ensured reliable data acquisition. These characteristics suggest the CuO NPs possess moderate colloidal stability and a broad size range suitable for catalytic, sensing, or biomedical use [59-62].

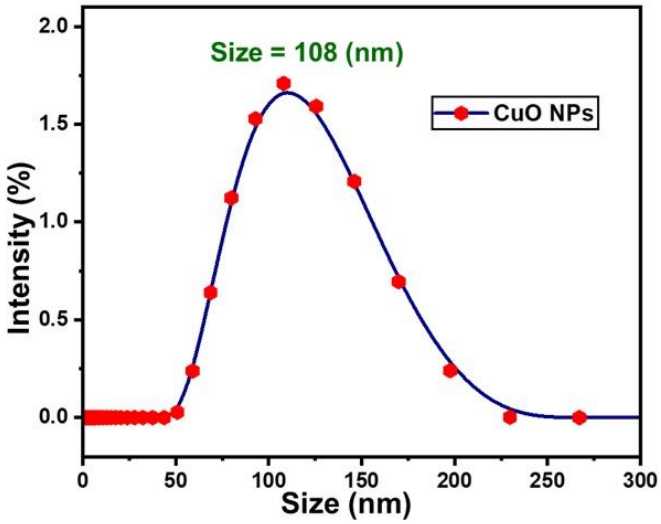


**Fig.6. DLS particles size analysis of CuO NPs**

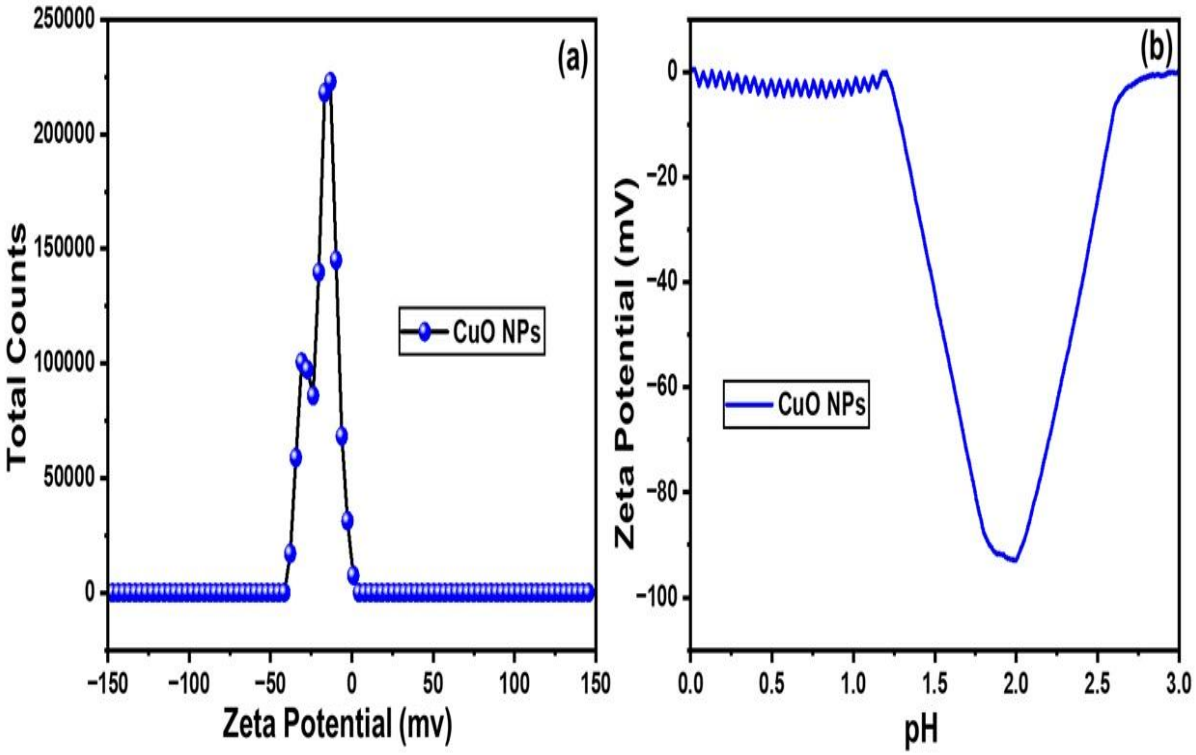


**Fig.7. Zeta-potential analysis of CuO NPs**

### 3.7. *In vitro* analysis of antidiabetic activity

The antidiabetic potential of the algal extract, CuO NPs, and starch/PVA/CuO-NPs nanoscaffolds was rigorously evaluated through standardized *in vitro* assays targeting key carbohydrate-digesting enzymes, α-amylase and α-glucosidase (Fig. 8). The results, derived from concentration-response studies (25-100 µg/mL), reveal distinct inhibitory profiles for each test material compared to the standard drug acarbose.

**α-Amylase inhibition:** Assessment using the DNSA method demonstrated clear concentration-dependent inhibition for all samples. The algal extract exhibited the weakest inhibitory activity across all tested concentrations. At the highest concentration (100 µg/mL), it achieved only 53.22% inhibition, significantly lower than acarbose (81.34%). CuO NPs displayed moderate activity, reaching 71.22% inhibition at 100 µg/mL. Notably, the starch/PVA/CuO-NPs nanoscaffolds exhibited the strongest activity among the test materials, closely approaching the efficacy of acarbose (80.22% vs 81.34% at 100 µg/mL). This pattern held across lower concentrations (25, 50, 75 µg/mL), where the nanoscaffolds consistently outperformed both the algal extract and the CuO NPs, though still slightly less effective than acarbose at 50 µg/mL and 75 µg/mL. A replicate assay generally confirmed these trends, showing the nanoscaffolds achieving 81.52% inhibition at 100 µg/mL compared to acarbose's 84.34% [63-66].

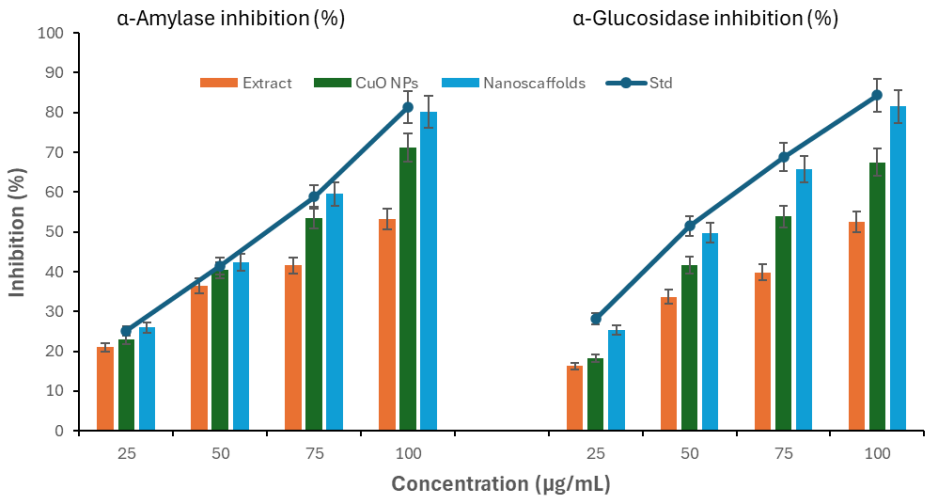


**Fig.8. Antidiabetic activity analysis of algal extract, CuNPs and starch/PVA/CuONPs nanoscaffolds**

**α-Glucosidase inhibition:** Evaluation via the pNPG substrate assay also showed concentration-dependent inhibition. Similar to the α-amylase results, the algal extract was the least effective inhibitor at all concentrations, achieving only 52.52% inhibition at 100 µg/mL in the first assay and replicating this level (52.52%) in the second assay. CuO NPs showed improved but still intermediate activity compared to the nanoscaffolds and standard (71.22% and 67.52% at 100 µg/mL in the two assays). The nanoscaffolds again demonstrated the highest potency among the novel test materials. Interestingly, in the second assay at 25 µg/mL, the nanoscaffolds (25.32%) even slightly surpassed the standard acarbose (28.13%). At higher concentrations in the glucosidase assay (50, 75, 100 µg/mL), the nanoscaffolds were highly effective but generally remained slightly below the inhibition levels achieved by acarbose, mirroring the pattern observed with α-amylase inhibition. For instance, at 100 µg/mL in the second assay, nanoscaffolds reached 81.52% inhibition versus acarbose's 84.34% [67-69].

The data unequivocally demonstrates that incorporating CuO NPs into the starch/PVA nanoscaffold matrix significantly enhances their antidiabetic enzyme inhibitory activity compared to either the raw algal extract or the CuO NPs alone. The nanoscaffolds consistently exhibited the strongest inhibition against both α-amylase and α-glucosidase among the tested novel materials, achieving efficacy levels remarkably close to, and occasionally exceeding at very low concentrations, the standard drug acarbose. This synergistic effect highlights the potential of the nanoscaffold formulation as a promising platform for developing antidiabetic therapeutics targeting carbohydrate digestion. The algal extract alone showed limited efficacy, while CuO NPs displayed moderate activity, significantly boosted upon integration into the nanoscaffold structure.

## 4. DISCUSSION

The present study systematically characterized the biosynthesized copper oxide (CuO) nanoparticles derived from *S. ilicifolium* extract and their integration into a starch/PVA nanofibrous scaffold. A comprehensive suite of analytical techniques was employed to confirm nanoparticle synthesis, structural incorporation, and biological efficacy, particularly focusing on their potential antidiabetic applications.

UV–Visible spectroscopy provided preliminary confirmation of nanoparticle formation through optical signatures characteristic of metal oxides. The distinct absorption peaks observed for the *S. ilicifolium* extract were attributable to its inherent phytoconstituents, likely including flavonoids and phenolic acids. In contrast, the synthesized CuO NPs exhibited prominent SPR bands, a hallmark of successful nanoparticle synthesis. These SPR bands arise due to collective oscillation of conduction band electrons at the nanoparticle surface when excited by light, suggesting the presence of well-dispersed CuO nanostructures. The measurement conditions were standardized for accuracy, and the baseline correction further validated the spectral integrity. The comparative analysis affirmed the transformation of the algal phytochemicals into a nanoparticulate form [70-72].

FTIR spectroscopy played a vital role in identifying the functional groups involved in nanoparticle synthesis and scaffold formation. The CuO NPs displayed distinct absorption bands linked to Cu–O vibrations, with additional peaks corresponding to hydroxyl, carbonyl, and possibly amine groups derived from phytochemicals. The electrospun starch/PVA scaffolds demonstrated bands typical of polysaccharide and polymer matrices, including O–H and C=O stretching vibrations. Shifts and broadening of absorption peaks in the composite scaffold suggested strong intermolecular interactions, likely hydrogen bonding or dipole interactions, between CuO NPs and the starch/PVA matrix. This interaction potentially contributes to the structural stability and controlled release behavior of the scaffold in biomedical environments [73-75].

XRD analysis offered insights into the crystalline nature and phase composition of the synthesized CuO NPs and the nanoscaffold. The CuO NPs exhibited sharp, well-defined peaks corresponding to the monoclinic phase of copper oxide, as matched with standard JCPDS data. The narrow full width at half maximum (FWHM) values

indicated a high degree of crystallinity, which is often associated with enhanced thermal and chemical stability. In contrast, the starch/PVA/CuO nanoscaffolds displayed broader peaks indicative of a semi-crystalline structure. This difference reflects the amorphous nature of the polymer matrix and successful nanoparticle incorporation without significant phase alteration. The composite material retained identifiable CuO peaks, confirming their structural integrity post-fabrication [76, 77].

Morphological examination via SEM revealed detailed surface characteristics and particle distribution. The CuO NPs appeared as aggregated, irregularly shaped entities, consistent with phytomediated synthesis processes where bioorganic molecules influence particle morphology. The starch/PVA nanoscaffolds demonstrated a homogenous, bead-free fibrous network with interconnected pores. Such architecture is desirable in biomedical scaffolds, facilitating cell adhesion, nutrient exchange, and controlled drug release. The integration of CuO NPs did not disrupt the fiber morphology, further supporting their compatibility and reinforcing the scaffold structure [78].

Thermal stability, a crucial parameter for biomedical applications, was evaluated using TGA. The starch/PVA/CuO nanoscaffolds demonstrated a two-step degradation pattern, with initial weight loss due to moisture evaporation, followed by polymer decomposition. The onset of degradation at over 230°C and completion near 374°C suggests that the scaffold maintains thermal integrity under physiological conditions. Incorporation of CuO NPs did not adversely affect thermal stability; instead, it may have contributed to enhanced decomposition resistance due to interaction with the polymer matrix [79].

Zeta potential and DLS analysis revealed critical information on the stability and size distribution of the nanoparticles. The CuO NPs exhibited a hydrodynamic diameter of 110 nm, placing them well within the optimal size range for cellular uptake and bioactivity. The moderate polydispersity index (PDI) suggests a relatively uniform size distribution, although further optimization may be required for large-scale biomedical applications. The zeta potential value of −18.3 mV indicates moderate colloidal stability, sufficient to prevent rapid aggregation, likely due to electrostatic repulsion imparted by surface-bound phytochemicals. These characteristics point to the CuO NPs being suitably stable for dispersion in aqueous environments [80].

The antidiabetic potential of the test materials was evaluated through inhibition of α-amylase and α-glucosidase enzymes, central to postprandial glucose regulation. Among the test samples, the starch/PVA/CuO nanoscaffolds consistently exhibited the most potent inhibitory activity, nearly paralleling that of the reference drug acarbose. The enhanced performance can be attributed to the synergistic interaction between CuO NPs and the polymeric matrix, which may have modulated the release and bioavailability of active sites. Interestingly, while the algal extract alone exhibited only modest inhibition, its bioactivity was markedly enhanced upon nanoparticle synthesis and scaffold incorporation. This suggests that the phytochemicals involved in CuO formation retain, and possibly potentiate, their biological activity in the nanoformulated state. Notably, the scaffolds demonstrated slightly higher inhibition than acarbose at lower concentrations in some assays, highlighting their promise for dose-efficient therapy [81].

Overall, the integrated physicochemical and biological assessments validate the successful synthesis of CuO NPs from *S. ilicifolium*, their effective embedding into starch/PVA nanoscaffolds, and the resulting composite's robust antidiabetic potential. The structural integrity, thermal resilience, morphological uniformity, and high enzyme inhibition activity collectively underscore the utility of this nanoscaffold system as a promising candidate for developing advanced antidiabetic therapeutics.

## 5. CONCLUSION

This study successfully demonstrated the green synthesis of CuO NPs using *S. ilicifolium* extract and their effective incorporation into starch/PVA electrospun nanoscaffolds. Comprehensive characterization using UV–Vis, FTIR, XRD, SEM, TGA, and DLS techniques confirmed the formation, structural integrity, and thermal stability of the synthesized nanomaterials. The nanoscaffolds exhibited a uniform fibrous network and good morphological properties, making them suitable for biomedical applications. Notably, *in vitro* enzyme inhibition assays revealed that the starch/PVA/CuO-NPs nanoscaffolds displayed significant antidiabetic activity by effectively inhibiting both α-amylase and α-glucosidase enzymes. The enhanced bioactivity compared to the algal extract and CuO NPs alone highlights a synergistic effect conferred by the nanoscaffold formulation. These findings suggest that the developed nanoscaffolds hold promising potential as a novel, sustainable therapeutic platform for managing diabetes. Further *in vivo* studies are warranted to validate their clinical relevance and expand their applicability in targeted drug delivery systems.

**Data Availability Statement:** The full dataset of physiochemical characterization associated with this work is published in Mendeley Data **[Dataset]** Innovative green composites: Material characterization of starch-based nanoscaffolds reinforced with *Sargassum ilicifolium*-mediated copper oxide nanostructures (DOI: 10.17632/4kdtskdtmc.2). Disclosure: The material characterization data and figures (e.g., UV, SEM, FTIR, XRD, TGA, Zeta Potential and particle sizer) presented here were generated from a common dataset and are being reused across multiple related studies on nanomaterials. All biological analyses and conclusions are original to each manuscript.

**Funding statement:** Not Available
**Conflicts of Interest:** The authors declare no conflicts of interest.
**Ethics approval statement:** Not Applicable

**REFERENCES**
[1] Sakthiraj A, Sivaramakrishnan R, Subramaniyam S, Kanniappan GV, Pandurangan V, Jayaraman S, Dhayalan VK, Mironescu M, Mironescu ID, Palanisamy CP. Starch/PVA electrospun nanoscaffolds loaded with ultrasonic-assisted green-synthesis of CuO nanoparticles from marine macroalgae (Gracilaria corticata) extract: Cytotoxicity and antioxidant analysis. Chemical Physics Impact. 2026; 12: 101018.
[2] Raju M, Chandrasekaran MK, Loganathan L, Ahalliya RM, Mironescu M, Mironescu ID, Palanisamy CP, Kanniappan GV. Lipid remodeling and ferroptosis in phosphatidylcholine-mediated tumor–stroma crosstalk. Frontiers in Molecular Biosciences. 2026; 13: 1742305.
[3] Kunamalla R, Panagal M, Palanisamy CP. Biogenic synthesis and fabrication of starch/PVA/CuO electrospun nanoscaffolds from Sargassum ilicifolium (brown marine macroalgae) extract for anticancer activity on HT-29 and MCF-7 cancer cells. Biocatalysis and Agricultural Biotechnology. 2026; 72: 103923.
[4] Pei J, Govindaraj H, Sivaramakrishnan R, Kanniappan GV, Pandurangan V, Dhayalan VK, Mironescu M, Mironescu ID, Jayaraman S, Palanisamy PC. Sustainable fabrication of biopolymer-based (starch/PVA) nanoscaffolds loaded with green-synthesized CuO nanoparticles from Sargassum wightii (marine macroalgae): Cytocompatibility and antioxidant activity. Biomaterials Advances. 2026; 182: 214660.
[5] Pei J, Perumal NC, Meng P, Long Q, Palanisamy CP. Extracellular vesicle-based biosensors for Alzheimer's disease: A new frontier in precision diagnostics. Ageing Research Reviews. 2026; 113: 102904.
[6] Shree P, Sivaramakrishnan R, Kanniappan GV, Pandurangan V, Jayaraman S, Dhayalan VK, Mironescu M, Mironescu ID, Palanisamy CP. Antioxidant and biocompatible CuO-starch/PVA nanoscaffolds via ultrasonic green synthesis using Turbinaria conoides (brown marine macroalgae). Medicine in Drug Discovery. 2025; 28: 100238.
[7] Gong J, Lin J, Guan T, Pei J, Palanisamy CP, El-AtyFrom AMA. selenium tolerance to nanoplastic antagonism: Comprehensive characterization of L. casei SNUT1 and its extracellular vesicle–nanoselenium complex. Food Bioscience. 2025; 74: 107749.
[8] Poochi SP, Sundarraj R, Raju MV, Chandrasekaran MK, Ahalliya RM, Palanisamy CP, Kanniappan GV, Kondapavuluri BK, Thiruvengadam M. Harnessing Nature: Computational and Experimental Insights Into *Ipomoea obscura* Metabolites for Bladder Cancer Therapy. Chemistry and Biodiversity. 2025; 0: e00909.
[9] Dugganaboyana GK, Kannankumar MKG, Shivaramakrishna S, Raju MV, Chandrasekaran MK, Ahalliya RM, Panneerselvam N, Palanisamy CP, Kanniappan GV. Phytochemical insights, antioxidant activity and therapeutic potential of Cassia senna against prostate cancer in Wistar albino rats. Discover Applied Sciences. 2025; 7:1206.
[10] Natarajan SR, Krishnamoorthy R, Alshuniaber MA, Gatasheh MK, Rajagopal P, Veeraraghavan VP, Palanisamy CP, Jayaraman S. KDM1A Facilitates Oncogenic Potential in Colorectal Cancer Progression Through the Activation of AXIN/GSK3β/β-Catenin Signaling Pathways: Evidence From Integrated Transcriptomics and In Vitro Studies. The Journal of Gene Medicine. 2025; 27(11): e70053.
[11] Guan T, Gong J, Lin J, Palanisamy CP, Jinjin Pei J, El-Aty AMA. Machine learning-driven multimodal optimization of selenium biotransformation and flavor profiling in fermented apple–Yacon functional beverages. Innovative Food Science & Emerging Technologies. 2025; 105: 104198.
[12] Natarajan SR, Krishnamoorthy R, Alshuniaber MA, Alsulami TS, Gatasheh MK, Rajagopal P, Palanisamy CP, Govindan R, Veeraraghavan VP, Jayaraman S. ABCE1 facilitates tumour progression via aerobic glycolysis and inhibits cell death in human colorectal cancer cells through the p53 signalling pathway. Scientific Reports. 2025; 15: 24674.
[13] Huang Y, Guo H, Liu Y, Jin W, Palanisamy CP, Pei J, Oz F, El-Aty AMA. Effects of Natural Polysaccharides on the Gut Microbiota Related to Human Metabolic Health. Molecular Nutrition & Food Research. 2025; 69:e202400792.
[14] Poornima K, Meenakshi K.C, Manikandan V.R, Shankari G, Prabhu D, Rathi M.A, Palanisamy CP, Balaji R, Gopalakrishnan V.K. Exploring the anticancer potential of Jerantinine A from *Tabernaemontana coronaria* against prostate, breast, and ovarian cancers: A computational approach. *Journal of Complementary and Integrative Medicine*, 2025 22(2): 363–372.
[15] Palanisamy CP, Poompradub S, Sansanaphongpricha K, Jayaraman S, Subramani K. Faridah Sonsudin gGreen synthesis of Nigella sativa-mediated silver nanoparticles for enhanced antibacterial activity and wound healing: Mechanistic insights and biomedical applications. Environmental Nanotechnology, Monitoring & Management. 2025; 24: 101085.
[16] Surendran N, Raju MV, Chandrasekaran MK, Ahalliya RM, Palanisamy CP, Chandrasekaran G, Kanniappan GV. Physicochemical characterization of starch from Maranta arundinacea L.(arrowroot) rhizomes and its inhibition of COX-2: In vivo validation. Bioactive Carbohydrates and Dietary Fibre. 2025; 33: 100465.
[17] Natarajan PM, Umapathy VR, Murali A, Swamikannu B. (2022). Computational Simulations of Identified marine-derived Natural Bioactive Compounds As Potential Inhibitors of Oral Cancer. Future Science OA. 2022; 8(3).

[18] Natarajan PM, Umapathy VR. Role of transcriptomics in the study of oral cancer. Frontiers in Oral Health. 2025; 6:1524364.
[19] Vidhyarekha U, Natarajan PM, Bhuminathan S, Sabarinathan J, Suba R, Vijayalakshmi P. Role of artificial intelligence in Oral Cancer. Advances in Public Health. 2024. 2024: 3664408.
[20] Ganesan A, Kumar NG, Natarajan PM, Gauthaman J. Automated classification of elongated styloid processes using deep learning models-an artificial intelligence diagnostics. Frontiers in Oral Health. 2025; 5: 1424840.
[21] Umapathy VR, Natarajan PM, Swamikannu B. Regenerative Strategies in Dentistry: Harnessing Stem Cells, Biomaterials and Bioactive Materials for Tissue Repair. Biomolecules. 2025; 15: 546.
[22] Natarajan PM. Dental Bioinformnatics-Current Scope and Future perspectives. Research Journal of Pharmacy and Technology. 2022;15(5):2351-6.
[23] Ganesan A, Kumar NG, Natarajan PM. Solanum trilobatum leaf extract-derived silver nanoparticles downregulate the PI3K/AKT/mTOR signaling pathway and attenuate oral squamous cell carcinoma cell proliferation. Journal of Herbmed Pharmacology. 2024; 13(2): 300-307.
[24] Perumal MKK, Renuka RR, Subbiah SK, Natarajan PM. Artificial intelligence-driven clinical decision support systems for early detection and precision therapy in oral cancer: a mini review. Frontiers in Oral Health. 2025; 6: 1592428.
[25] Ramesh E, Ganesan A, Lakshmi KC, Natarajan PM. Artificial intelligence-based diagnosis of oral leukoplakia using deep convolutional neural networks Xception and MobileNet-v2. Frontiers in Oral Health. 2025; 6: 1414524.
[26] Ganesan A, Kumar NG, Natarajan PM. Anticancer activity of silver nanoparticles synthesized from aqueous leaf extract of Solanum trilobatum (Purple fruit pea eggplant) on human oral cancer cells. Journal of Herbmed Pharmacololgy. 2024; 13(2): 260-268.
[27] Pei JJ, Perumal NC, Meng P, Long Q, Palanisamy CP. AI-assisted FTIR spectroscopic profiling of exosomes: Emerging frontiers in early detection of Alzheimer's disease. Ageing Research Reviews. 2026; 103311.
[28] Raja FSD, Abraham L, Rangasamy K, Saikia K, Rathankumar AK, Mironescu M, Mironescu I, Palanisamy CP, Kanniappan GV. Next-Generation Microbiome Therapeutics: Psychobiotics and Fecal Microbiota Transplants (FMT) for Mental Health Treatment. Frontiers in Cellular and Infection Microbiology. 2026; 16: 1719357.
[29] Subramani K, Srinivasan S, Shanmugam P, Palanisamy CP, Sonsudin F, Poompradub S. Sustainable phytochemical mediated-ZnO nanoparticles derived from Crescentia cujete for toxicological evaluation and multifunctional environmental applications. Environmental Nanotechnology, Monitoring & Management. 2026; 26: 101180.
[30] Kunamalla RP, Panagal M, Palanisamy CP. Green-engineered multiscale starch/PVA nanofibrous scaffolds embedded with CuO nanoparticles from Sargassum ilicifolium for potent antimicrobial performance. Genetics and Molecular Research. 2026; 25(13s): 1-9.
[31] Dharmaprakash S, Gunasekaran VP, Sivaramakrishnan R, Kanniappan GV, Jayaraman S, Mironescu M, Rajabathar JR, Mironescu ID, Palanisamy CP. Marine macroalgae-mediated ultrasonic-assisted green synthesis of CuO nanoparticles embedded in starch/PVA electrospun nanoscaffolds for in vitro α-amylase and α-glucosidase inhibitory activity. Scientific Reports. 2026; 16: 26243.
[32] Surendran N, Chandrasekaran G, Raju MV, Chandrasekaran MK, Ahalliya RM, Palanisamy CP, Kanniappan GV, Arcot R, Alharbi NS, Thiruvengadam M. Anti-inflammatory potential of ethanolic extract of Maranta arundinacea L.: Insights from COX-2 modulation and oxidative stress analysis. South African Journal of Botany. 2026; 195: 142-151.
[33] Pei J, Senthilkumar MV, Hessini K, Subramaniyam S, Sivaramakrishnan R, Kanniappan GV, Jayaraman S, Palanisamy CP. Green fabrication of starch/PVA/CuO nanoscaffolds using marine macroalgae extract for enhanced anti-inflammatory activity. Sustainable Chemistry and Pharmacy. 2026; 51: 102397.
[34] Balasubramanian V, Loganathan L, Muthuswamy K, Viswanathan TM, Raju MV, Chandrasekaran MK, Ahalliya RM, Poorasamy J, Palanisamy CP, Dominic S, Kanniappan GV. Anticancer therapeutic efficacy of PEGylated β-galactosidase from Aspergillus terreus in DMBA-induced breast cancer: Toxicological, molecular and histopathological evaluation in Wistar rats. International Journal of Biological Macromolecules. 2026; 360: 151856.
[35] Jayaraman S, Eswaran A, Rajagopal P, Palanisamy CP, Veerakumar P, Veeraraghavan VP, Sirasanagandla SR. Neuroendocrine-associated epigenetic factors in cellular senescence: mechanisms and therapeutic implications. Biogerontology. 2026; 27(2): 64.
[36] Jayakumar M, Senthil P, Suganthirababu P, Ramalingam V, Palanisamy CP. Longitudinal effects of body weight supported gait training on functional gait recovery after stroke: A pilot randomized controlled trial. Genetics and Molecular Research. 2026; 25(12s): 2026.
[37] Ponnusamy B, Rajagopal P, Palanisamy CP, Veeraraghavan VP, Jayaraman S. Mechanistic Exploration of the anticancer activity of Justicia adhatoda Plant Leaf Ethanolic Extract against Colon Cancer Cells: An in silico and in vitro Approach. Asian Pacific Journal of Cancer Prevention. 2026; 27(3): 1069-1080.
[38] Pei J, Saran VS, Sivaramakrishnan R, Kanniappan GV, Pandurangan V, Jayaraman S, Dhayalan VK, Mironescu M, Mironescu ID, Palanisamy CP. Ultrasonic-assisted, Sargassum ilicifolium (brown marine

macroalgae)-mediated biogenic synthesis of CuO nanoparticles incorporated in starch/PVA electrospun nanoscaffolds: In vitro safety and antioxidant efficacy assessment. Bioorganic Chemistry. 2026; 173: 109679.
[39] Raj MAPA, Subramaniyam S, Kanniappan GV, Jayaraman S, Palanisamy CP. Sustainable fabrication of starch/PVA/CuO electrospun nanoscaffolds from Turbinaria ornata (marine macroalgae) extract: Physicochemical characterization and antidiabetic evaluation. Kuwait Journal of Science. 2026; 53(2): 100545.
[40] Pei J, Ganesh NS, Subramaniyam S, Sivaramakrishnan R, Kanniappan GV, Jayaraman S, Palanisamy CP. Sustainable fabrication of starch/PVA/CuO electrospun nanoscaffolds from Padina tetrastromatica (Brown macroalgae) extract: Physicochemical characterization and antidiabetic assessment. Sustainable Chemistry One World. 2026; 9: 100195.
[41] Natarajan PM, Swamikannu B, Sivaraman NM, Stylin AGSQ. Prevention of Oral Cancer: A Comprehensive Guide. Journal of Pharmacy and Bioallied Sciences. 2024; 16(5): S4239-S4241.
[42] Umapathy V, Dhanavel A, Kesavan R, Natarajan PM, Bhuminathan S, Vijayalakshmi P. Anticancer Potential of the Principal Constituent of Piper nigrum, Piperine: A Comprehensive Review. Cureus. 2024; 16(2): e54425.
[43] Umapathy VR, Swamikannu B, Natarajan PM, Devi R, Nandini MS, Vimalarani, Vijayalakshmi P. In Silico Molecular Docking of Ocimum sanctum Phytochemicals: Targeting Key Biomarkers in Oral Cancer. Journal of Pharmacy and Bioallied Sciences. 2024; 16(5): S4792-S4799.
[44] Natarajan PM, Bhuminathan S, Rajan R, Bindu K, Loganathan K, Veerakumar R. The Crucial Role of Smoking Cessation in Preventing Oral Cancer. Journal of Pharmacy and Bioallied Sciences. 2024; 16(5): S4245-S4247.
[45] Swamikannu B, Umapathy VR, Natarajan PM, Nandini MS, Stylin AGSQ, Vimalarani V, Rajinikanth S. Unlocking the Therapeutic Benefits of Artemisia Annua: A Comprehensive Overview of its Medicinal Properties. Journal of Pharmacy and Bioallied Sciences. 2024; 16(5): S4248-S4253.
[46] Natarajan PM. Computational Studies on Recent Congeners of Fluoroquinolones and Nitroimidazoles for Their Use in Periodontal Therapy. Journal of Pharmacy and Bioallied Sciences. 2024; 16(5): S4731-S4740.
[47] Yadalam PK, Arumuganainar D, Natarajan PM, Ardila CM. Artificial intelligence-powered prediction of AIM-2 inflammasome sequences using transformers and graph attention networks in periodontal inflammation. Scientific Reports. 2025; 15: 8733.
[48] Yadalam PK, Chatterjee S, Natarajan PM, Ardila CM. Comparison of light gradient boosting and logistic re gression for interactomic hub genes in Porphyromonas gingivalis and Fusobacterium nucleatum-induced periodo ntitis with Alzheimer's disease. Frontiers in Oral Health. 2025; 6:1463458.
[49] Natarajan PM, Bhuminathan S, Leela B, Bindu K, Loganathan K, Ramachandran V. Smoking and its Role in Oral Cancer. Journal of Pharmacy and Bioallied Sciences 16(5): S4242-S4244.
[50] Yadalam PK, Natarajan PM, Ardila CM. Variational graph autoencoder for reconstructed transcriptomic data associated with NLRP3 mediated pyroptosis in periodontitis. Scientific Reports. 2025; 15: 1962.
[51] Kannappan P, Chandrasekaran MK, Raju MV, Gopalakrishnan S, Dhamodharan P, Ahalliya RM, Palanisamy CP, Raju B, Kanniappan GV. Exploring the anticancer potential of Jerantinine A from Tabernaemontana coronaria against prostate, breast, and ovarian cancers: a computational approach. Journal of Complementary and Integrative Medicine. 2025; 22(02): 363-372.
[52] Pei J, Kumarasamy RV, Jayaraman S, Kanniappan GV, Long Q, Palanisamy CP. Quercetin-functionalized nanomaterials: Innovative therapeutic avenues for Alzheimer's disease management. Ageing Research Reviews. 2025; 104: 102665.
[53] Jayaraman S, Prasad M, Natarajan SR, Krishnamoorthy R, Alshuniaber MA, Gatasheh MK, Veeraraghavan VP, Rajagopal P, Palanisamy CP. Molecular mechanisms underlying the effects of beta-sitosterol on TGF-β1/Nrf2/SIRT1/p53-mediated signaling in the kidney of a high-fat diet and sucrose-induced type-2 diabetic rat. Chemico-Biological Interactions. 2025; 411: 111443.
[54] Huang Y, Guo H, Liu Y, Jin W, Palanisamy CP, Pei J, Oz F, El-Aty AMA. Effects of Natural Polysaccharides on the Gut Microbiota Related to Human Metabolic Health. Molecular Nutrition & Food Research. 2025; e202400792.
[55] Prabhakaran P, Palanisamy CP, Shanmugam A, Damodharan P, Swaminathan H, Devaraj D, Ahalliya RM, Kanniappan GV. Isolation, structural characterization, and molecular docking studies on the bioactive compound from n-Hexane extract of Emilia sonchifolia (L.) DC against the pancreatic cancer target Aurora 2 Kinase. Journal of Complementary and Integrative Medicine. 2024; 22(1): 0290.
[56] Jiang H, Kumarasamy RV, Pei J, Raju K, Kanniappan GV, Palanisamy CP. Integrating engineered nanomaterials with extracellular vesicles: Advancing targeted drug delivery and biomedical applications. Frontiers in Nanotechnology. 2024; 6: 1513683.
[57] Guo H, Liu Y, Wan T, Song D, Palanisamy CP, Geng J, Pei J, Özmen S, El-Aty AMA. Toward personalized cancer management: Role of precision nutrition–diet interventions. Journal of Functional Foods. 2024; 123: 106584.
[58] Natarajan SR, Krishnamoorthy R, Alshuniaber MA, Al-Anazi KM, Farah MA, Rajagopal P, Palanisamy CP, Veeraraghavan VP, Jayaraman S. Identification of FOXM1 as a novel protein biomarker and therapeutic target for colorectal cancer progression: Evidence from immune infiltration and bioinformatic analyses. International Journal of Biological Macromolecules. 282 (Part 4): 137201.

[59] Rajendran MS, Jayaraman S, Khan JM, Jasmine S, Prabhakaran RK, Raju MV, Chandrasekaran MK, Ahalliya RM, Kannappan P, Palanisamy CP, Kanniappan GV. Investigating the colon toxicity and carcinogenic role of monosodium glutamate compared with Dimethylhydrazine in male Wistar rats: Exploring the link to childhood colon cancer risk. Journal of King Saud University - Science. 2024; 36(11): 103507.
[60] Kumarasamy RV, Natarajan P, Umapathy VR, Roy JR, Rab SO, Saeed M, Panagal M, Mironescu M, Srinivasan GP, Palanisamy CP. Clinical Applications and Therapeutic Potentials of Advanced Nanoparticles: A Comprehensive Review on Completed Human Clinical Trials. Frontiers in Nanotechnology. 2024; 6:1479993.
[61] Jin W, Pei JJ, Roy JR, Jayaraman S, Ahalliya RM, Kanniappan GV, Mironescu M, Palanisamy CP. Comprehensive review on single-cell RNA sequencing: A new frontier in Alzheimer's disease research. Ageing Research Reviews. 2024; 274: 102454.
[62] Pei J, Palanisamy CP, Jayaraman S, Natarajan PM, Umapathy VR, Roy JR, Panagal M, Jayaraman S. Curcumin-loaded polymeric nanomaterials as a novel therapeutic strategy for Alzheimer's disease: A comprehensive review. Ageing Research Reviews. 2024; 99: 102393.
[63] Pei J, Palanisamy CP, Jayaraman S, Natarajan PM, Umapathy VR, Roy JR, Thalamati D, Ahalliya RM, Kanniappan GV, Mironescu M. A comprehensive review on starch-based Sustainable Edible Films Loaded with Bioactive Components for Food Packaging. International Journal of Biological macromolecules. 2024; 274 (Part-1): 133332.
[64] Palanisamy CP, poompradub S, Sansanaphongpricha K, Subramani K, Sonsudin F. Increased expression levels of PDGF and VEGF magnify the wound healing potential facilitated by biogenic synthesis of silver nanoparticles. Nano-Structures & Nano-Objects. 2024; 39: 101236.
[65] Pei J, Palanisamy CP, Jayaraman S, Natarajan PM, Umapathy VR, Roy JR, Thalamati D, Ahalliya RM, Kanniappan GV, Mironescu M. Proteomics Profiling of Extracellular Vesicle for Identification of Potential Biomarkers in Alzheimer's Disease: A Comprehensive Review. Ageing Research Reviews. 2024; 99: 102359.
[66] Xi J, Wang T, Xian P, Liu X, Du M, Yang H, Palanisamy CP, Lin W, Long Q. Proteomic insights uncover enhanced neurotherapeutic potential in conditioned mesenchymal stem cell-derived extracellular vesicles. Extracellular Vesicle. 2024; 3: 100037.
[67] Pei J, Natarajan PM, Umapathy VR, Swamikannu B, Sivaraman NM, Krishnasamy L, Palanisamy CP. Advancements in the synthesis and functionalization of zinc oxide-based nanomaterials for enhanced oral cancer therapy. Molecules. 2024; 29(11): 2706.
[68] Gatasheh MK, Natarajan SR, Krishnamoorthy R, Alsulami TS, Rajagopal P, Palanisamy CP, Veeraraghavan VP, Jayaraman S. Molecular analysis to identify novel potential biomarkers as drug targets in colorectal cancer therapy: an integrated bioinformatics analysis. Molecular and Cellular Oncology. 2024; 11(1): 2326699.
[69] Pei J, Yan Y, Jayaraman S, Rajagopal P, Natarajan PM, Umapathy VR, Gopathy S, Roy JR, Sadagopan CS, Thalamati D, Palanisamy CP, Mironescu M. A review on advancements in the application of starch-based nanomaterials in biomedicine: Precision drug delivery and cancer therapy. International Journal of Biological Macromolecules. 2024; 130746.
[70] Pei JJ, Yan Y, Palanisamy CP, Jayaraman S, Natarajan PM, Umapathy VR, Gopathy S, Roy JR, Sadagopan JC, Thalamati D, Mironescu M. Materials-based drug delivery approaches: Recent advances and future perspectives. Green Processing and Synthesis. 2024; 13: 20230094.
[71] Pei JJ, Deng W, Liu Y, Guo Y, Chen J, Abdu H, Khan MR, Palanisamy CP, El-Aty AM. A Comprehensive Review of Cornus officinalis: Health Benefits, Phytochemistry, and Pharmacological Effects for Functional Drug and Food Development. Frontiers in Nutrition. 2023; 10: 1309963.
[72] Alugoju P, Palanisamy CP, Anthikapalli NVA, Jayaraman S, Prasanskulab A, Chuchawankul S, Dyavaiah M, Tencomnao T. Exploring the anti-aging potential of natural products and plant extracts in budding yeast Saccharomyces cerevisiae: A review. F1000Research. 2023; 12: 1265.
[73] Lavanya M, Krishnamoorthy R, Alshuniaber MA, Manoharadas S, Palanisamy CP, Veeraraghavan VP, Jayaraman S, Rajagopal P, Padmini R. Formulation, characterization and evaluation of gelatin-syringic acid/zinc oxide nanocomposite for its effective anticancer, antioxidant and anti-inflammatory activities. Journal of King Saud University-Science. 2023; 35: 102909.
[74] Palanisamy CP, Poompradub S, Sansanaphongpricha K, Jayaraman S, Subramani K, Sonsudin F. Biosynthesis of silver nanoparticles (AgNPs) using ethanolic extract of Nigella sativa (L.) seeds promotes wound healing via PDGF and VEGF signalling pathways activation. Biocatalysis and Agricultural Biotechnology. 2023; 54: 102970.
[75] Prasad M, Jayaraman S, Natarajan SR, Veeraraghavan VP, Krishnamoorthy R, Gatasheh MK, Palanisamy CP, Elrobh M. Piperine modulates IR/Akt/GLUT4 pathways to mitigate insulin resistance: Evidence from animal and computational studies. International Journal of Biological Macromolecules. 2023; 253: 127242.
[76] Palanisamy CP, Pei JJ, Phaniendra A, Venkata AAN, Jayaraman S, Veeraragahavan VP, Sridevi G, Roy JR, Janaki CS, Thalamati D, Mironescu M, Luo Q, Chai Y, Long Q. New Strategy of Neurodegenerative Disease Treatment with Extracellular Vesicles (EVs) Derived from Mesenchymal Stem Cells (MSCs). *Theranostics*. 2023; 13(12):4138-4165. doi:10.7150/thno.83066.
[77] Palanisamy CP, Phaniendra A, Jayaraman S, Poompradub S. *Nigella sativa* L. seed extracts promotes wound healing progress by activating VEGF and PDGF signalling pathways: *An in vitro* and *in silico* study. *F1000 Research*. 2023; 12: 436.

[78] Pei JJ, Palanisamy CP, Phaniendra A, Venkata AAN, Natarajan PM, Umapathy VR, Swamikannu B, Jayaraman S, Rajagopal P, Poompradub S. A comprehensive review on bio-based materials for chronic diabetic wounds. *Molecules*. 2022; 28(2), 604.
[79] Palanisamy CP, Cui B, Zhang H, Gunasekaran VP, Ariyo A, Jayaraman S, Veeraraghavan V, Rajagopal P. A critical review on starch-based electrospun nanofibrous scaffolds for wound healing application. International Journal of Biological Macromolecules. 2022; 222 (Part: B): 1852-1860.
[80] Monisha P, Ponnulakshmi R, Nalini D, Vishnu P V, Palanisamy CP, Cui B, Shankargouda P, Selvaraj J. A comprehensive review on high fat diet-induced diabetes mellitus: An epigenetic view. The Journal of Nutritional Biochemistry. 2022; 2022: 109037.
[81] Monisha P, Selvaraj J, Mohamed AE, Mohamed E, Mosaab AEA, Vishnu PV, Srinivasan V, Vidhya RU, Shazia FJH, Kalaiselvi K, Durairaj S, Palanisamy CP, Surapaneni K M, Ponnulakshmi R. A Comprehensive review on therapeutic perspectives of phytosterols in insulin resistance: A mechanistic approach. Molecules. 2022; 27(5): 1595.